Applied Surface Science 256 (2010) 2726–2730

Contents lists available at ScienceDirect

Applied Surface Science

journal homepage: www.elsevier.com/locate/apsusc

Deposition and properties of B–N codoped *p*-type ZnO thin films by RF magnetron sputtering

Y.R. Sui [a,b], B. Yao [a,c,*], J.H. Yang [b], H.F. Cui [a], X.M. Huang [a], T. Yang [a], L.L. Gao [a], R. Deng [a], D.Z. Shen [c]

[a] Department of Physics, Jilin University, Changchun 130023, China
[b] Department of Physics, Jilin Normal University, Siping 136000, China
[c] Changchun Institute of Optics, Fine Mechanics and Physics, Chinese Academy of Sciences, Changchun 130033, China

ARTICLE INFO

Article history:
Received 25 May 2009
Received in revised form 26 October 2009
Accepted 7 November 2009
Available online 13 November 2009

Keywords:
Zinc oxide
B–N codoping
p-Type conduction
Sputtering
Properties

ABSTRACT

B–N codoped *p*-type ZnO thin films have been realized by radio frequency (rf) magnetron sputtering using a mixture of argon and oxygen as sputtering gas. Types of conduction and electrical properties in codoped ZnO films were found to be dependent on oxygen partial pressure ratios in the sputtering gas mixture. When oxygen partial pressure ratio was 70%, the codoped ZnO film showed *p*-type conduction and had the best electrical properties. Additionally, the *p*-ZnO/*n*-Si heterojunction showed a clear *p*–*n* diode characteristic. XRD results indicate that the B–N codoped ZnO film prepared in 70% oxygen partial pressure ratio has high crystal quality with (0 0 2) preferential orientation. Meanwhile, the B–N codoped ZnO film has high optical quality and displays the stronger near band edge (NBE) emission in the temperature-dependent photoluminescence spectrum, the acceptor energy level was estimated to be located at 125 meV above the valence band.

1. Introduction

ZnO is a II–VI compound semiconductor with a wide direct band gap of 3.37 eV at room temperature [1]. It has an exciton binding energy of 60 meV larger than that of GaN and high exciton emission efficiency. Due to these features, ZnO has become a promising candidate for applications in blue and ultraviolet (UV) light sources and as a UV detector [2–5]. Its practical applications in these fields depend on the fabrication of ZnO *p*–*n* homojunctions. However, making reliable and reproducible *p*-type ZnO is still a bottleneck, which impedes the practical application of ZnO-based devices. The difficulty is mainly due to the self-compensation effect of native defects and the low solubility limit of acceptor dopants [6,7]. Thus recent effort in ZnO research has been focused on the synthesis of *p*-type ZnO using various techniques and dopants [8]. It has been suggested that *p*-type doping in ZnO can be achieved by substituting either group-I elements, such as Li, Na and K, for Zn sites or group-V elements, like N, P, As and Sb, for O sites [9–15].

Among these possible dopants for *p*-type ZnO, N is thought to be a promising candidate, which has a similar ionic radius as oxygen [9,16]. But various efforts to realize this goal have been frustrated, such as the reactive evaporation [17], and radio frequency sputtering [18]. It can be attributed that N monodoping (MD) creates a rather deep acceptor level, which is unfavorable for successful doping. On the other hand, the low solubility of N MD may not create a sufficient number of holes to compensate the free electrons in order to obtain *p*-type ZnO [19]. However, the codoping method using acceptor (e.g., N) and donors (e.g., B, Al, Ga, or In) simultaneously was suggested theoretically as a possible means to enhance nitrogen solubility in ZnO and to lower its ionization energy [20–22]. Recently experimental investigation related to the codoping techniques, such as Al–N [23,24], Ga–N [25,26], and In–N [27,28] has also appeared in several literatures. However, no successful preparation of *p*-type ZnO using B–N codoping method was reported so far.

In this present work, *p*-type ZnO films were prepared using the B–N codoping by rf magnetron sputtering in Ar–O_2 ambient. The effect of oxygen partial pressure ratios on electrical properties of codoped films was reported. Moreover, structural and optical properties of B–N codoped *p*-type ZnO film were studied.

2. Experimental details

Two series of films, B–N codoped and undoped ZnO films, were prepared on quartz substrates by rf magnetron sputtering technique. The target for codoped films was prepared by sintering mixture of ZnO (99.99% purity) and 1 at.% BN (99.99% purity) powders at 1000 °C for 10 h in air ambient. The target for undoped

* Corresponding author at: Department of Physics, Jilin University, Changchun 130023, China. Tel.: +86 0431 86176355; fax: +86 0431 86171688.
E-mail address: binyao@jlu.edu.cn (B. Yao).

0169-4332/$ – see front matter © 2009 Elsevier B.V. All rights reserved.
doi:10.1016/j.apsusc.2009.11.017

film was prepared by sintering ZnO (99.99% purity) powders at 1000 °C for 10 h in air ambient. The quartz substrates were cleaned in an ultrasonic bath with acetone, ethanol, and de-ionized water at room temperature, and then washed using de-ionized water. The vacuum chamber was evacuated to a base pressure of 5×10^{-4} Pa, then filled with flow of mixed gases (99.99% pure argon and oxygen) up to 1.0 Pa, and this pressure was maintained during the growing process. The oxygen concentration in the mixed gases is described by the oxygen partial pressure ratio, which is defined as the oxygen partial pressure divided by the total pressure of 1.0 Pa, which can be changed from 0% to 100%. The gas pressure ratio can be turned by controlling flow rates of oxygen and argon. The sputtering power was 120 W. The films were grown on the quartz for 1 h at substrate temperature of 773 K by rf magnetron sputtering, then annealed for 30 min at 873 K under 10^{-4} Pa in a tube furnace. To prevent pollution, a quartz tube was inserted into the furnace and the films were placed in a quartz boat.

The structures of the films were characterized by rotation anode X-ray diffractometer (XRD) (Rigaku D/Max-RA) with Cu $K\alpha_1$ radiation ($\lambda = 0.15406$ nm), the scan step size used is 0.02°, and error is within ±0.0003 nm for lattice constant measurement. Electrical properties were measured in the van der Pauw configuration by a Hall effect measurement system at room temperature. The depth profiles of B, N, Zn and O were measured by Time-of-Flight secondary-ion mass spectrometry (TOF-SIMS). Photoluminescence measurement was performed at room temperature by the excitation from a 325 nm He–Cd laser. Raman spectra were excited by radiation of 514.5 nm from a Renishaw inVia Raman spectrometer. In order to avoid the heating of the sample, the incident power was limited at 20 mW.

3. Results and discussion

The electrical properties of codoped ZnO films as a function of oxygen partial pressure ratios are shown in Fig. 1. The films deposited in 0% and 30% of oxygen partial pressure ratios showed *n*-type conduction. The dependence of conduction type on oxygen partial pressure ratio suggests that the concentration of native defects, such as oxygen vacancies (V_O) or zinc interstitials (Zn_i), is more than that of active acceptors for the films deposited in low oxygen partial pressure ratios. Hence, *n*-type conduction was observed. As the oxygen partial pressure ratio further increases, the concentration of V_O decreased and the concentration of Zn vacancies (V_{Zn}) increased. Enhancement of V_{Zn} may facilitate the substitution of B for the sites of Zn atoms in the ZnO crystal lattice, which possibly leads to the formation of the bonds of B–N. Therefore, nitrogen atoms have been doped into the ZnO films as acceptor dopants, which substitute for oxygen in ZnO crystal lattice, when the concentration of active acceptors exceeds the donor concentration, the conduction type changes from *n*- to *p*-type. This is probably the main reason for the better *p*-type electrical properties of this stage. When oxygen partial pressure ratio increased to 70%, the film showed the best electrical properties with the lowest resistivity of 2.3 Ω cm, Hall mobility of 15 $cm^2/V\,s$ and carrier concentration of 1.2×10^{17} cm^{-3}. When oxygen partial pressure ratio increases continually, some nitrogen in ZnO crystal lattice may be substituted by oxygen because oxygen is more active than nitrogen. Therefore, concentration of holes carries decreased, correspondingly the resistivity increased.

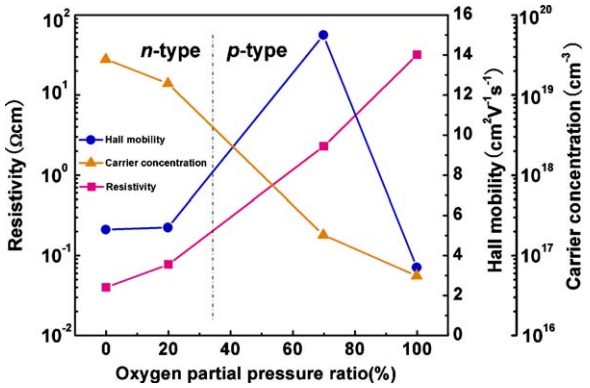

Fig. 1. Effect of oxygen partial pressure ratios on the conduction type, carrier concentration, mobility and resistivity of B–N codoped ZnO films deposited on quartz substrate.

In order to understand the effect of B–N codoping on ZnO films properties, an undoped ZnO film was grown on a quartz substrate by sputtering of the pure ZnO target with sputtering gas of argon and oxygen under the same experimental conditions as B–N codoping ZnO film. Table 1 shows the electrical properties of undoped and B–N codoped ZnO films deposited in 70% of oxygen partial pressure ratio. Hall measurement indicates that when oxygen partial pressure ratio is 70%, the undoped ZnO film exhibits *n*-type conduction, and the codoped film shows *p*-type conduction, the low resistivity of 2.3 Ω cm, high carrier concentration of 1.2×10^{17} cm^{-3} and high hall mobility of 15 $cm^2/V\,s$ were acquired at room temperature. As a result, we can conclude that the acceptable *p*-type ZnO film has been prepared by the codoping of boron and nitrogen. It can be explained that under 70% of oxygen partial pressure ratio sputtering ambient, the concentration of oxygen vacancies decreased and the concentration of V_{Zn} increased. Enhancement of V_{Zn} may facilitate the substitution of B for the sites of Zn atoms in the ZnO crystal lattice, which leads to the formation of the bonds of B–N. Therefore, nitrogen atoms substitute for oxygen as acceptor dopants in ZnO crystal lattice, so that the incorporation of N atoms as acceptors take part in the hole conductivity.

Fig. 2 shows the XRD patterns of the undoped and B–N codoped ZnO films deposited in 70% of oxygen partial pressure ratio. Both ZnO films have high film quality with (0 0 2) preferential orientation. No other phases (e.g., BN, or Zn_3N_2) are detected. Compared with the undoped ZnO film, the intensity of the (0 0 2) peak somewhat decreases and its full-width at half-maximum (FWHM) increases from 0.33° to 0.36° for the B–N codoped film. This may be due to the incorporation of both B and N dopants into the ZnO film can create more defects in the lattice, which indicate degrading crystallinity somewhat. Moreover, the diffraction angle of the (0 0 2) peak shifts to higher diffraction angle from 34.45° to 34.51° and the d-spacing value decreases from 2.603 to 2.599 Å. In addition, the lattice constant obtained from the (2 0 0) diffraction peak for undoped film is 5.206 Å, while the lattice constant obtained from B–N codoped ZnO film is 5.199 Å. The variation is attributed to the substitution of B for the sites of Zn atoms in the ZnO crystal lattice and N atoms substitute for O atoms and become an acceptor [29], which leads to the formation of the bonds of B–N in B–N codoped ZnO film. Since B–N bond length is somewhat smaller than Zn–O bond length, therefore, d-spacing value and the lattice constant for codoped ZnO film became smaller than that of undoped ZnO film, which agrees with high diffraction angle. That is in consistent with the hall measurement result.

Secondary-ion mass spectroscopy (SIMS) was used to verify the presence of B and N in the B–N codoped ZnO film. The depth profile of B, N, Zn and O in the B–N codoped ZnO film deposited in 70% of oxygen partial pressure ratio is shown in Fig. 3. It is evident that B and N have been clearly detected, and theirs concentration profiles are quite flat throughout the film depth. This indicates that B and N have been doped into the ZnO film with a uniform distribution, which contributes to the good crystalline quality and *p*-type conductivity of the B–N codoped ZnO film. In addition, the film

Table 1
The electrical properties of the B–N codoped and undoped ZnO films deposited in 70% of oxygen partial pressure ratio at room temperature.

Sample	Resistivity (Ω cm)	Carrier concentration (cm^{-3})	Mobility ($cm^2 V^{-1} s^{-1}$)	Type
B–N codoped film	2.3	1.8E+17	15	*p*
Undoped film	9.5E+1	9.5E+15	7.3	*n*

thickness can be estimated from the SIMS profile curve to be about 700 nm.

In order to prove the existing of B–N bond in the B–N codoped ZnO film, Raman spectroscopy measurements were performed for undoped and B–N codoped ZnO films deposited in 70% of oxygen partial pressure ratio, as shown in Fig. 4(a) and (b), respectively. In Fig. 4(a), the peaks at 437, 488, 584 cm^{-1} are assigned to the optical phonon modes of the ZnO film [30–32]. The peak at about 794 cm^{-1} is related to the quartz substrate [32]. The peak approximately positioned at 584 cm^{-1} is ascribable to the formation of the defects, such as oxygen vacancy, interstitial Zn, and lack of the free carrier [32]. Differing from Fig. 4(a), the 584 cm^{-1} peak disappears and an additional Raman peak at 1065 cm^{-1} is observed in Fig. 4(b). The disappearance of the 584 cm^{-1} peak implies that the defects such as oxygen vacancies and Zn interstitial decreased, and the free carrier increased in the B–N codoped ZnO film, compared to the undoped ZnO film. The latter is in consistent with the hall measurement result. It is well known that frequency of an optical phonon mode of B–N bond is 1058 cm^{-1} in BN with zinc blende structure [33], which is close to the frequency of the additional Raman peak located at 1065 cm^{-1}. Therefore, the 1065 cm^{-1} peak is attributed to local vibration mode of B–N bond in the B–N codoped ZnO. The frequency shift may be caused by the difference of B–N bond surrounding chemical environment. Similar phenomenon is also found in In–N codoped ZnO [34]. This implies that covalent B–N bond exists in the B–N codoped ZnO film.

In order to further understand the *p*-type behavior of B–N codoped ZnO films deposited in 70% of oxygen partial pressure ratio. The *I–V* characteristic of the *p*-ZnO/*n*-Si heterojunction at room temperature is shown in Fig. 4. The lower right inset shows the schematic structure of the *p–n* heterojunction for *I–V* measurement. The *p*-type ZnO layer was grown directly on the *n*-Si. Indium electrodes were used to form Ohmic contacts to the *n*-type layer and Ni/Au electrodes were used to form Ohmic contacts to the *p*-type layer. The upper left inset shows the Ohmic contact characteristic of two Ni/Au contacts on the *p*-ZnO and two In contacts on the *n*-Si. The linear *I–V* curves for both Ni/Au on *p*-ZnO and In on *n*-Si reveal that good Ohmic contacts have been obtained for both electrodes. As can be seen, *I–V* curves of the *p–n* heterojunction exhibit typical rectification behavior of a *p–n* diode, indicating that *p*-type conduction was indeed achieved.

Based on groups III–V elements codoping theory [20] and experimental results mentioned above, the formation mechanism of the B–N codoped *p*-type ZnO films is suggested. For the B–N codoped ZnO, the ratio of N to B is 2:1, and the B occupies Zn site (B_{Zn}) and N does O site (N_O). One N atom occupies O site which is the nearest neighbor with B atom, forming B–N pair, which conduction contribution will be zero, and another N is located at the next-nearest-neighbor site of the B in a layer closest to the layer including the B–N pair, due to the strong repulsive interaction between the N acceptors, forming N_O acceptor. The *p*-type conductivity mainly comes from the contribution of the N_O acceptor for the B–N codoped *p*-type ZnO film.

Fig. 5 shows the 83 K PL spectra of B–N codoped *p*-type ZnO film deposited in 70% of oxygen partial pressure ratio, which exhibits clearly resolved emission at 3.352, 3.312, 3.235, and 3.163 eV. The upper left inset shows the temperature-dependent PL spectra of the B–N codoped *p*-type ZnO film. The peak at 3.352 eV can be assigned to an acceptor bound exciton (A^0X) [35]. The emission peak at 3.312 eV can be attributed to the conduction band to acceptor transition (or free electrons to the acceptor (FA) transition) as reported in In–P codoped ZnO [36]. However, the peak at 3.235 and 3.163 eV is assigned to donor–acceptor pair (DAP) transition and its longitudinal optical (LO) phonon replicas of DAP–LO with a periodic spacing of ~72 meV, respectively, which is identical with the results for GaN codoped *p*-type ZnO [37]. Moreover, DAP emission is observed at 3.238 eV for *p*-type N-doped ZnO [38]. It can be concluded that the FA transition and the DAP transition related to acceptors were brought as a result of acceptor being nitrogen on an oxygen site. The depth of the nitrogen acceptor relative to the valence band can be evaluated as the difference between the band gap and the FA transition, which is given by

$$E_A = E_{gap} - E_{FA} + \frac{k_B T}{2}$$

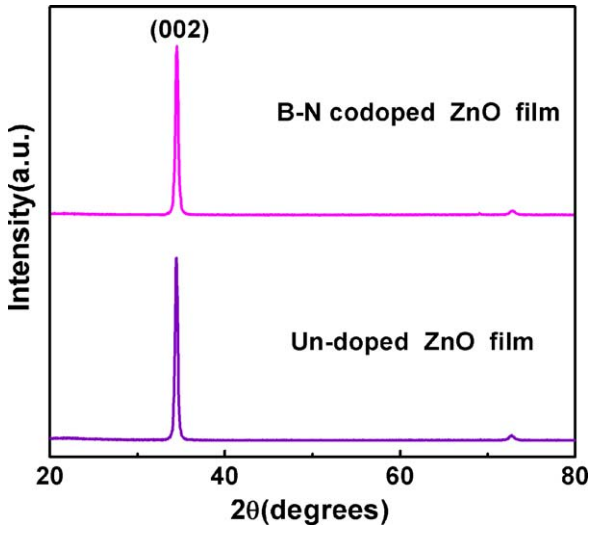

Fig. 2. X-ray diffraction patterns of the undoped and B–N codoped ZnO films deposited in 70% of oxygen partial pressure ratio on quartz substrate.

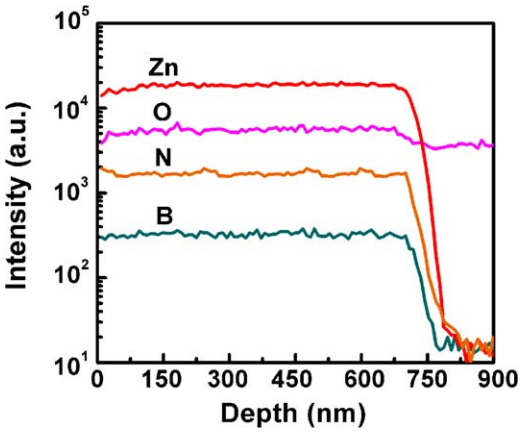

Fig. 3. SIMS depth profiles of B–N codoped ZnO film deposited in 70% of oxygen partial pressure ratio.

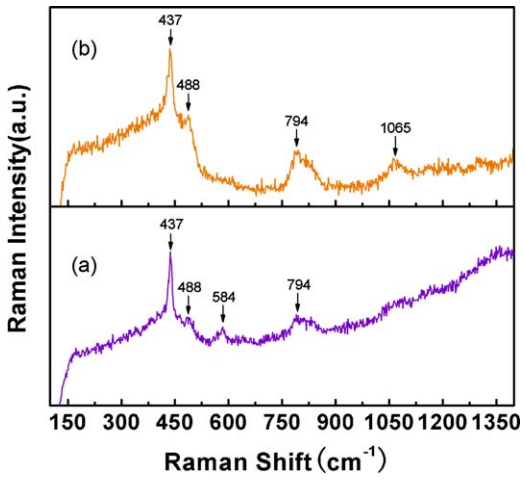

Fig. 4. Raman spectra of the (a) undoped and (b) B–N codoped ZnO films deposited in 70% of oxygen partial pressure ratio on quartz substrate.

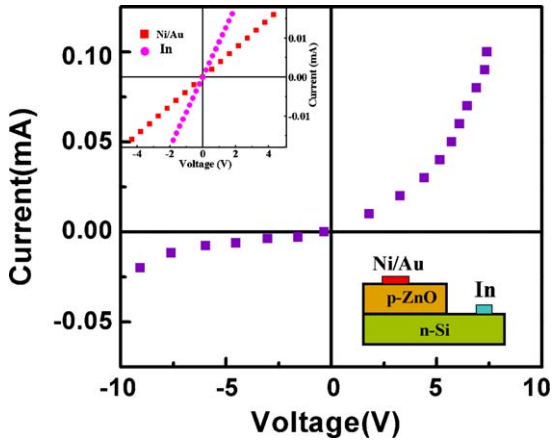

Fig. 5. The *I*–*V* characteristic of the *p*-ZnO/*n*-Si heterojunction. The upper left inset shows the Ohmic contact characteristic of two Ni/Au contacts on the *p*-ZnO and two In contacts on the *n*-Si. The lower right inset shows the schematic structure of the *p*–*n* heterojunction.

where E_{gap} and E_{FA} are the band gap and FA transition energies, respectively. Since the thermal energy term can be neglected at low temperature, therefore, the optical binding energy of nitrogen acceptors can be estimated from the above equation $E_A = E_g$ (3.437 eV [39]) − E_{FA} (3.312 eV) + (k_BT/2) = 125 meV. A value of 125 meV for E_A is in agreement with the value of 119 meV obtained in our other B–N codoped ZnO films deposited in N_2–O_2 ambient. The acceptor energy levels of N-doped *p*-type ZnO are reported in the range of 170–200 meV at a 9×10^{16} cm^{-3} hole concentration [38]. The shallow acceptor energy level of 125 meV suggests that the use of B–N codoping as dopants in ZnO would be very desirable, in terms of obtaining a high hole concentration in *p*-type ZnO.

4. Conclusions

In summary, B–N codoped *p*-type ZnO films were fabricated on quartz substrate by rf magnetron sputtering using mixture of argon and oxygen as sputtering gas. Types of conduction and electrical properties in codoped ZnO films were found to be dependent on oxygen partial pressure ratios in the sputtering gas mixture. When oxygen partial pressure ratio was 70%, the codoped ZnO film showed *p*-type conduction and had the best electrical properties, which showed a resistivity of 2.3 Ω cm with a Hall mobility of 15 cm^2/V s and carrier concentration of 1.8×10^{17} cm^{-3}. In addition, the *p*-type

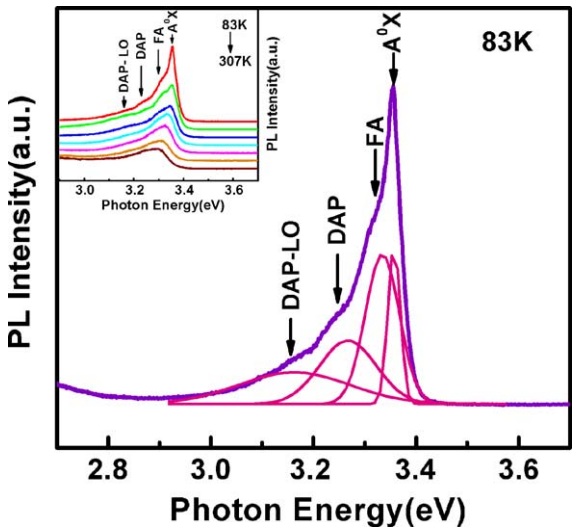

Fig. 6. The 83 K PL spectra of B–N codoped *p*-ZnO films deposited in 70% of oxygen partial pressure ratio on quartz substrate. The upper left inset shows the temperature-dependent PL spectra of the B–N codoped *p*-type ZnO film measured at temperature from 83 to 307 K.

behavior of B–N codoped ZnO films deposited in 70% of oxygen partial pressure ratio was confirmed by *p*-ZnO/*n*-Si heterojunction which showed a clear *p*–*n* diode characteristic. The 83 K PL spectra revealed that for the codoped *p*-type ZnO film there were UV emission peaks at 3.353, 3.312, 3.235, and 3.163 eV, respectively (Fig. 6). The acceptor energy level was estimated to be located 125 meV above the valence band. Our results show that codoping of boron and nitrogen should be a good way to prepare *p*-type ZnO.

Acknowledgements

The authors would like to thank financial support of the Key Project of National Natural Science Foundation of China under Grant No. 50532050, the "973" program under Grant No. 2006CB604906, the Innovation Project of Chinese Academy of Sciences, the National Natural Science Foundation of China under Grant Nos. 6077601, 60506014, 10674133, 60806002 and 10874178.

References

[1] C. Klingshirn, Phys. Stat. Sol. B 71 (1975) 547.
[2] Z.K. Tang, G.K.L. Wong, P. Yu, Appl. Phys. Lett. 72 (25) (1998) 3270.
[3] D.M. Bagnall, Y.F. Chen, Z. Zhu, T. Yao, Appl. Phys. Lett. 73 (8) (1998) 1038.
[4] R.K. Thareja, A. Mitra, Appl. Phys. B 71 (2000) 181.
[5] T. Makino, C.H. Chia, T.T. Nguen, Y. Segawa, Appl. Phys. Lett. 77 (11) (2000) 1632.
[6] S.B. Zhang, S.H. Wei, A. Zunger, Phys. Rev. B 63 (2001) 075205.
[7] E.C. Lee, Y.S. Kim, Y.G. Jin, K.J. Chang, Phys. Rev. B 64 (2001) 085120.
[8] D.C. Look, Semicond. Sci. Technol. 20 (2005) S55.
[9] C.H. Park, S.B. Zhang, S.H. Wei, Phys. Rev. B 66 (2002) 073202.
[10] T.M. Barnes, K. Olson, C.A. Wolden, Appl. Phys. Lett. 86 (2005) 112112.
[11] F.X. Xiu, Z. Yang, L.J. Mandalapu, J.L. Liu, W.P. Beyermann, Appl. Phys. Lett. 88 (2006) 052106.
[12] D.C. Look, G.M. Renlund, R.H. Burgener II, J.R. Sizelove, Appl. Phys. Lett. 85 (2004) 5269.
[13] F.X. Xiu, Z. Yang, L.J. Mandalapu, D.T. Zhao, J.L. Liu, Appl. Phys. Lett. 87 (2005) 252102.
[14] K. Nakahara, H. Takasu, P. Fons, A. Yamada, K. Iwata, K. Matsubara, R. Hunger, S. Niki, Appl. Phys. Lett. 79 (2001) 4139.
[15] J.G. Lu, Y.Z. Zhang, Z.Z. Ye, L.P. Zhu, L. Wang, B.H. Zhao, Q.L. Liang, Appl. Phys. Lett. 88 (2006) 222114.
[16] A. Kobayashi, O.F. Sankey, J.D. Dow, Phys. Rev. B 28 (1983) 946.
[17] Y. Sato, S. Sato, Thin Solid Films 281 (1996) 445.
[18] A. Valentini, F. Quaranta, M. Rossi, G. Battaglin, J. Vac. Sci. Technol. A 9 (1991) 286.
[19] L.G. Wang, A. Zunger, Phys. Rev. Lett. 90 (2003) 256401.
[20] T. Yamamoto, H. Katayama-Yoshida, Jpn. J. Appl. Phys. Part 2 38 (1999) L166.
[21] T. Yamamoto, Phys. Stat. Sol. A 193 (3) (2002) 423.
[22] T. Yamamoto, Jpn. J. Appl. Phys. 42 (2003) 514.

[23] J.G. Lu, Z.Z. Ye, F. Zhuge, Y.J. Zeng, B.H. Zhao, L.P. Zhu, Appl. Phys. Lett. 85 (2004) 3134.
[24] G.D. Yuan, Z.Z. Ye, L.P. Zhu, Q. Qian, B.H. Zhao, R.X. Fan, Appl. Phys. Lett. 86 (2006) 202106.
[25] M. Joseph, H. Tabata, T. Kawai, Jpn. J. Appl. Phys. Part 2 38 (1999) L1205.
[26] M. Kumar, T.H. Kim, S.S. Kim, B.T. Lee, Appl. Phys. Lett. 89 (2006) 112103.
[27] J.M. Bian, X.M. Li, X.D. Gao, W.D. Yu, L.D. Chen, Appl. Phys. Lett. 84 (2004) 541.
[28] L.L. Chen, J.G. Lu, Z.Z. Ye, Y.M. Lin, B.H. Zhao, Y.M. Ye, J.S. Li, L.P. Zhu, Appl. Phys. Lett. 87 (2005) 252106.
[29] X.N. Li, B. Keyes, S. Asher, S.B. Zhang, S.H. Wei, T.J. Coutts, S. Limpijumnong, C.G. Van der Walle, Appl. Phys. Lett. 86 (2005) 122107.
[30] Y. Huang, M. Liu, Z. Li, Y. Zeng, S. Liu, Mater. Sci. Eng. B 97 (2003) 111.
[31] D. Behera, B.S. Acharya, J. Lumin. 128 (2008) 1577.
[32] S.B. Yahia, L. Znaidi, A. Kanaev, J.P. Petitet, Spectrochim. Acta Part A 71 (2008) 1234.
[33] A.I. Lukomskii, V.B. Shipilo, E.M. Shishonok, Phys. Stat. Sol. 102 (1987) 137.
[34] J.F. Kong, H. Chen, H.B. Ye, W.Z. Shen, J.L. Zhao, X.M. Li, Appl. Phys. Lett. 90 (2007) 041907.
[35] J. Gutowski, N. Presser, I. Broser, Phys. Rev. B 38 (1988) 9746.
[36] J.D. Ye, S.L. Gu, F. Li, S.M. Zhu, R. Zhang, Y. Shi, Y.D. Zheng, X.W. Sun, G.Q. Lo, D.L. Kwong, Appl. Phys. Lett. 90 (2007) 152108.
[37] H. Wang, H.P. Ho, K.C. Lo, K.W. Cheah, J. Phys. D: Appl. Phys. 40 (2007) 4682.
[38] D.C. Look, D.C. Reynolds, C.W. Litton, R.L. Jones, D.B. Eason, G. Cantwell, Appl. Phys. Lett. 81 (2002) 1830.
[39] B.K. Meyer, Phys. Stat. Sol. B 241 (2004) 231.